

Interference Level Estimation for a Blind Source Separation in Document Restoration

Antonio Boccuto[1], Ivan Gerace[1(✉)], and Valentina Giorgetti[2]

[1] Dipartimento di Matematica e Informatica, via Vanvitelli, 1, 06123 Perugia, Italy
{antonio.boccuto,ivan.gerace}@unipg.it
[2] Dipartimento di Matematica e Informatica,
viale G. B. Morgagni 67/A, 50134 Firenze, Italy
valentina.giorgetti@unifi.it

Abstract. We deal with the problem of blind separation of the components, in particular for documents corrupted by bleed-through and show-through. So, we analyze a regularization technique, which estimates the original sources, the interference levels and the blur operators. We treat the estimate of the interference levels, given the original sources and the blur operators. In particular, we investigate several GNC-type algorithms for minimizing the energy function. In the experimental results, we find which algorithm gives more precise estimates of the interference levels.

Keywords: Blind source separation · Image restoration · Document restoration · Bleed-through · Show-through · GNC technique

1 Introduction

In this paper we deal with a *Blind Source Separation* (BSS) problem for the analysis of digital documents. Digital imaging for documents is very important, because it allows to have digital achieves, to make always possible the accessibility and the readability. The *Digital Document Restoration* consists of a set of processes finalized to the visual and aesthetic improvement of a virtual reconstruction of a corrupted document, without risk of deterioration.

We deal with *show-through* and *bleed-through* effects. The show-through is a front-to-back interference, caused by the transparency of the paper and the scanning process, and by means of which the text in the one side of the document can appear also in the other side. The bleed-through is an intrinsic front-to-back physical deterioration caused by ink seeping, and its effect is similar to that of show-through. The physical model for the show-through effect has to take into account the spreading of light in the paper, the features of the paper, the reflectance of the verso and the transmittance parameters, and so, in general, it turns to be rather complicated. In [20], G. Sharma gave a nonlinear mathematical model which was first analyzed and then further approximated so to become

© The Author(s), under exclusive license to Springer Nature Switzerland AG 2022
O. Gervasi et al. (Eds.): ICCSA 2022, LNCS 13375, pp. 428–444, 2022.
https://doi.org/10.1007/978-3-031-10522-7_30

easier to handle. A nonlinear modified Sharma model is proposed in [12,17,19]. In particular, in [12] it is proved that the results given there by the nonlinear model improve those obtained by means of data decorrelation or independent component analysis. In [17] a cost function is introduced, which includes the non-linear model together with a regularization term related to Total Variation. In [19] the interference levels are estimated a priori and then an iterative procedure is used for the estimates of the recto and verso of documents. Some nonlinear models which assume that the interference levels depend on the location are presented in [9,11,22]. So, the model turns to be non-stationary, that is not translation invariant. The algorithms in [9,22] for the resolution of the related inverse problem are fast heuristics. In [4], a non-stationary model is proposed. However, in order to obtain more precise results, a computationally more expensive regularized problem has been sketched in [8] and [21]. Now we analyze in detail the iterative technique to solve such a model, in which the sources, the blur operators and the interference level are computed separately at every step, until a fixed point is found. In this paper, in particular, we deal with determining the interference levels, by fixing the blur operators and the ideal sources. To this aim, we use a GNC-type technique (see, e.g., [1–3,5,6,10,13–16,18]). Note that a correct estimate of the interference levels is crucial in our approach for a right recognition of the letters in documents.

In this paper we analyze four different GNC-type algorithms to determine the interference level. Such algorithms are experimentally compared, and we have chosen the algorithm which has given estimates of the interference levels closest to ideal levels, improving the results presented in [8] and [21].

In a forthcoming paper, the steps about finding the blur operators and the ideal sources will be treated.

The paper is structured as follows. In Sect. 2 we deal with the regularization of the modified Sharma model. In Sect. 3 we describe the alternating iterative algorithm, used to find the minimum of the energy function. In Sect. 4 we analyze the technique to determine the interference levels, given the blur operator and the ideal sources. In Sect. 5 we propose different types of convex approximations. In Sect. 6 we present GNC-type alternative minimization techniques. In Sect. 7 we compare the proposed technique by means of the experimental results.

2 Regularization of the Problem

In this paper we consider a modified Sharma-type model related to the show-through phenomenon in paper documents, as follows (see, e.g., [8,21]):

$$r^d(i,j = r(i,j)e^{q_v(i,j)\left(\frac{z_v(i,j)}{N}-1\right)},\ v^d(i,j) = v(i,j)e^{q_r(i,j)\left(\frac{z_r(i,j)}{N}-1\right)}, \qquad (1)$$

where N is the maximum value of the light intensity, which is assumed to correspond with the background of the analyzed document; $r = [r(i,j)]$, $v = [v(i,j)] \in \mathbb{R}^{nm}$ are the vectors which represent the ideal images of the recto and the verso of the document (expressed in the lexicographic form); $q_r(i,j)$ is the interference

level which affects the light intensity of interferences from the recto to the verso; $q_v(i,j)$ is the interference level which affects the light intensity of interferences from the verso to the recto; $r^d = [r^d(i,j)], v^d = [v^d(i,j)] \in \mathbb{R}^{nm}$ are the vectors which represent the observed data mixtures (expressed in the lexicographic form); $z_r = [z_r(i,j)] = Af, z_v = [z_v(i,j)] = Ar$ are the blurred images of the recto and the verso, where $A \in \mathbb{R}^{(nm)\times(nm)}$ is the blur operator, which in general has the form of a matrix with Toeplitz blocks. The problem of the blind separations of components consists of finding an estimate of the recto/verso pair of the source document, which is denoted by $s = (r, v)$, of the interference level $q = (q_r, q_v)$ and of the blur operator A, given as input the observed images of the recto and the verso. This is an ill-posed problem in the Hadamard sense. To estimate the solution of the problem, some regularization techniques are used. Thus, the solution of the regularized problem is $(s^*, q^*, A^*) = \arg\min_{(s,q,A)} E(s,q,A)$, where

$$E(s,q,A) = T(s,q,A) + \widehat{S}(s) + S(q_r) + S(q_v) + S_c(q_r,q_v) \tag{2}$$

is the *energy function*, and

$$T(s,q,A) = T_r(q_v) + T_v(q_r) = \sum_{i=1}^{n}\sum_{j=1}^{m}\left(r^d(i,j) - r(i,j)\mathrm{e}^{-q_v(i,j)\left(1-\frac{z_v(i,j)}{N}\right)}\right)^2 + \sum_{i=1}^{n}\sum_{j=1}^{m}\left(v^d(i,j) - v(i,j)\mathrm{e}^{-q_r(i,j)\left(1-\frac{z_r(i,j)}{N}\right)}\right)^2 \tag{3}$$

is the *consistency term*, which measures the faithfulness of the solution to the data, and $\widehat{S}(s)$ is the *regularization term*, which is chosen according to the properties which the estimated source has to satisfy. Moreover, the last terms of (2) are given by

$$S(q_w) = \lambda_w^2 \sum_{i=1}^{n}\sum_{j=1}^{m}\left[\Big(q_w(i,j) - q_w(i-1,j)\Big)^2 + \Big(q_w(i,j) - q_w(i,j-1)\Big)^2\right],$$

where $w \in \{r, v\}$, λ_w is the regularization parameter related to the interference level of the recto (resp. verso), if $w = r$ (resp., $w = v$), and

$$S_c(q_r,q_v) = \sum_{i=1}^{n}\sum_{j=1}^{m}\lambda_c^2(q_r(i,j) - q_v(i,j))^2$$

is the joint smoothness term. The parameter λ_c is the regularization parameter between the interference of the recto and the verso with respect to the same pixel.

3 Alternating Techniques

To minimize the function in (2), we use a strategy of *alternating minimization*, which consists of the estimation of the minimum of the function with respect to each single variable, fixing the other ones. We proceed as follows:

initialize $k = 0$, s_0, q_0, A_0
while a stationary point of E is not found
$k = k + 1$
$s_k = \arg\min_s E(s, q_{k-1}, A_{k-1})$
$q_k = \arg\min_q E(s_{k-1}, q, A_{k-1})$
$A_k = \arg\min_A E(s_{k-1}, q_{k-1}, A)$

To solve the problem of minimization of the dual energy, which in general is not convex, a technique introduced by Blake and Zisserman can be used (see, e.g., [1–3,5,6,10,13–16,18]). With such a technique, called GNC (*Graduate Non-Convexity*), the energy function E, is approximated by means of a finite family $\{E^{(p)}\}$ of functions, in such a way that the first one is convex and the last one coincides with the given function. Moreover, we call $\mathbf{x}$ the variable with respect to which we will compute the minimum of E. The algorithm is structured as follows: every energy function is minimized by starting with the minimum achieved by optimizating the approximation of the energy function obtained at the previous step. By choosing different approximating functions, it is possible to obtain various formulations of the GNC algorithm. The minimization of each of the approximating functions $E^{(p)}$ can be done by means of an algorithm called NL-SOR (*Non Linear Successive Over-Relaxation*) (see, e.g., [7]).

4 Determining the Interference Levels

In this paper, we deal with finding only the interference levels, fixed the recto, the verso and the blur mask. The other steps of the alternating algorithm will be treated in a forthcoming paper. The energy function with respect to the interference level is given by

$$E(s_{k-1}, q, A_{k-1}) = k + \sum_{i=1}^{n}\sum_{j=1}^{m}\left(r^d(i,j) - r(i,j)\mathrm{e}^{-q_v(i,j)\left(1-\frac{z_v(i,j)}{N}\right)}\right)^2 \tag{4}$$

$$+\sum_{i=1}^{n}\sum_{j=1}^{m}\left(v^d(i,j) - v(i,j)\mathrm{e}^{-q_r(i,j)\left(1-\frac{z_r(i,j)}{N}\right)}\right)^2 + S(q_r) + S(q_v) + S_c(q_r, q_v),$$

where $k = \widehat{S}(s_{k-1})$ is a constant. It is possible to prove that the smoothness terms are convex. Now, define $\psi : \{v, r\} \to \{v, r\}$ by

$$\psi(r) = v, \quad \psi(w) = r. \tag{5}$$

It is not difficult to see that the Hessian matrix of the data consistency term is positive-definite if and only if

$$q_w(k,t) < -\frac{\ln\left(\frac{(\psi(w))^d(k,t)}{2\,\psi(w)(k,t)}\right)}{1-\frac{z_w(k,t)}{N}} \quad \text{for all } w \in \{r, v\},\ k \in \{1, \ldots, n\},\ t \in \{1, \ldots, m\}.$$

Thus, the energy function related to the interference level is given by the sum of the terms of data consistency, which are not necessarily convex, and the smoothness terms, which are convex. Hence, in general the uniqueness of the global minimum is not guaranteed.

5 Convex Approximation of the Data Consistency Term

To approximate the term of faithfulness to the data, it is possible to approximate T_v and T_r separately. Moreover, we can approximate each term of the sum in (3) separately too. Fixed $i \in \{1,\dots,n\}$, $j \in \{1,\dots,m\}$ and $v \in \{f,r\}$, let ψ be as in (5), and denoting by $\alpha = \dfrac{\psi(w)(i,j)}{\psi(w^d)(i,j)}$, $\gamma = \dfrac{z_w(i,j)}{N} - 1$, $q = q_w(i,j)$, the term related to the faithfulness to the data can be expressed as

$$\begin{aligned} T(s,q,A) = T_r(q_v) + T_v(q_r) &= \sum_{i=1}^{n}\sum_{j=1}^{m}\left(r^d(i,j) - r(i,j)\mathrm{e}^{-q_v(i,j)\left(1-\frac{z_v(i,j)}{N}\right)}\right)^2 \\ &+ \sum_{i=1}^{n}\sum_{j=1}^{m}\left(v^d(i,j) - v(i,j)\mathrm{e}^{-q_r(i,j)\left(1-\frac{z_r(i,j)}{N}\right)}\right)^2 \qquad (6) \\ &= \sum_{i=1}^{n}\sum_{j=1}^{m}\sum_{w\in\{r,v\}} \psi(w)^d(i,j)\,\varphi_{i,j,w}(q), \end{aligned}$$

where

$$\varphi_{i,j,w}(q) = \left(1 - \alpha\ e^{q\gamma}\right)^2 = 1 - 2\alpha\ e^{q\gamma} + \alpha^2\ e^{2q\gamma}. \qquad (7)$$

Therefore, to make the function $\varphi_{i,j,w}$ in (7) convex, we will proceed in several ways. In particular, in this paper we approximate the quantity $g_{i,j,w}(q) = e^{q\gamma}$ by a line of the type $\tilde{g}(q) = \tilde{A}\,q + \tilde{B}$. So, the approximation of $\varphi_{i,j,w}(q)$ is given by $\tilde{\varphi}(q) = (1 - \alpha\tilde{A}\,q - \tilde{B})^2$, which is a convex function.

5.1 Interpolating Approximation

Now we approximate $g_{i,j,w}(q)$ with the line $p^{(1)}_{i,j,w}(q)$ interpolating at the points $(3, e^{3\gamma})$ and $(0,1)$. It is not difficult to see that

$$p^{(1)}_{i,j,w}(q) = q\left(\frac{e^{3\gamma}}{3} - \frac{1}{3}\right) + 1.$$

Thus, the convex approximation of $\varphi_{i,j,w}(q)$ is given by

$$\varphi^{(1)}_{i,j,w}(q) = \left(1 - \alpha\, q\frac{e^{3\gamma}-1}{3} - \alpha\right)^2. \qquad (8)$$

5.2 The Best Line Approximation

Now we approximate $g_{i,j,w}(q)$ by the line $p^{(2)}_{i,j,w}(q)$ of best approximation with respect to the 2-norm in $P_1([0,3]) = \{p : [0,3] \to \mathbb{R} |\ p$ is a polynomial of degree at most $1\}$. It is not difficult to see that (Figs. 1, 2)

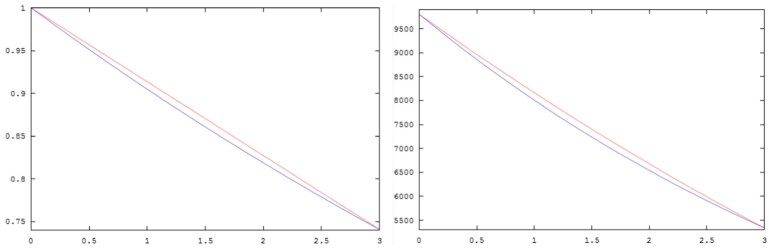

Fig. 1. On the left side: Graph of $g_{i,j,w}(q)$ in blue and $p^{(1)}(q)$ in red. On the right side: Graph of $\varphi_{i,j,w}(q)$ in blue and $\varphi^{(1)}(q)$ in red ($\alpha = 100$, $\gamma = 0.1$). (Color figure online)

$p^{(2)}_{i,j,w}(q) = A^{(2)}\, q + B^{(2)}$, where

$$A^{(2)} = \frac{2}{3\,\gamma}\Big(2e^{3\gamma} - \frac{2(e^{3\gamma}-1)}{3\,\gamma} - e^{3\gamma} + 1\Big),$$
$$B^{(2)} = -\frac{5\,e^{3\gamma}}{3\,\gamma} - \frac{4}{3\,\gamma} + \frac{2\,e^{3\gamma}}{3\,\gamma^2} - \frac{2}{3\,\gamma^2} + \frac{e^{3\gamma}}{\gamma}.$$

The convex approximation of $\varphi_{i,j,w}(q)$ is

$$\varphi^{(2)}_{i,j,w}(q) = \Big(1 - \alpha\, A^{(2)}\, q - B^{(2)}\Big)^2. \tag{9}$$

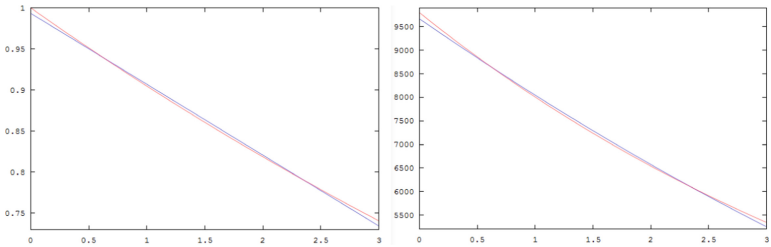

Fig. 2. On the left side: Graph of $g_{i,j,w}(q)$ in blue and $p^{(2)}(q)$ in red. On the right side: Graph of $\varphi_{i,j,w}(q)$ in blue and $\varphi^{(2)}(q)$ in red ($\alpha = 100$, $\gamma = 0.1$). (Color figure online)

Note that this is the first convex approximation chosen in the GNC-type algorithm proposed in [8] and [21].

5.3 Hybrid Best Approximation and Interpolation

Now we approximate $g_{i,j,w}(q)$ by means of the line $p^{(5)}_{i,j,w}(q)$ of best approximation related to the 2-norm in $P_1([0,3]) = \{p : [0,3] \to \mathbb{R} |\ p$ is a polynomial of degree at most $1\}$, which interpolates $g_{i,j,w}(q)$ at a chosen point $\bar{q}$. (Figs. 3, 4)

Now we make a change of coordinates, in such a way that the "new" origin coincides with $(\bar{q}, g_{i,j,w}(\bar{q}))$. Let us define

$$\tilde{g}(q) = g_{i,j,w}(q + \bar{q}) - g_{i,j,w}(\bar{q}). \tag{10}$$

Note that $\tilde{g}$ is a translation of $g_{i,j,w}$ in the Cartesian plane. Now we determine the polynomial $\tilde{p}^{(5)}$ of best approximation of $\tilde{g}$ with respect to the 2-norm in

$$P_1([-\bar{q}, 3-\bar{q}]) = \{p : [-\bar{q}, 3-\bar{q}] \to \mathbb{R} \mid p \text{ is a polynomial of degree at most } 1\}$$

which interpolates $\tilde{g}$ at 0. We use the Gram-Schmidt method to find an orthonormal basis $\{e_1\}$ of the space $\{p \in P_1([-\bar{q}, 3-\bar{q}]) | \, p(0) = 0\}$. A basis for this space is given by $x_1 = q$. By normalizing, we get

$$||x_1|| = \sqrt{\int_{-\bar{q}}^{3-\bar{q}} q^2 \, dq} = \sqrt{3}\,(\sqrt{\bar{q}^2 - 3\bar{q} + 3}),$$

So, the normalized basis is given by

$$e_1 = \frac{x_1}{||x_1||} = \frac{q\sqrt{3}}{3(\sqrt{\bar{q}^2 - 3\bar{q} + 3})}.$$

The polynomial $\tilde{p}^{(5)}(q)$ of best approximation of $\tilde{g}_{i,j,w}(q)$ is

$$\tilde{p}^{(5)}(q) = c_1 e_1(q),$$

where $c_1 = < \tilde{g}, e_1 >$ is equal to

$$-\frac{\sqrt{3}}{3(\sqrt{\bar{q}^2 - 3\bar{q} + 3})} e^{\bar{q}\gamma} \left(\frac{(\bar{q} - 3)e^{(3-\bar{q})\gamma} - \bar{q}\, e^{-\bar{q}\gamma}}{\gamma} + \frac{e^{(3-\bar{q})\gamma} - e^{-\bar{q}\gamma}}{\gamma^2} + \frac{9 - 6\bar{q}}{2} \right).$$

By taking the inverse translation, we obtain

$$p^{(5)}_{i,j,w}(q) = \tilde{p}^{(5)}(q - \bar{q}) + g_{i,j,w}(\bar{q}) = A^{(5)}(\bar{q})\, q + B^{(5)}(\bar{q}),$$

where

$$\begin{aligned} A^{(5)}(\bar{q}) = &-\frac{e^{\bar{q}\gamma}}{6(\bar{q}^2 - 3\bar{q} + 3)} \left(\frac{(2\bar{q} - 6)e^{(3-\bar{q})\gamma} - 2\bar{q}\, e^{-\bar{q}\gamma}}{\gamma} \right. \\ &\left. + \, 2\frac{e^{(3-\bar{q})\gamma} - e^{-\bar{q}\gamma}}{\gamma^2} + 9 - 6\bar{q} \right), \\ B^{(5)}(\bar{q}) = &\frac{\bar{q}\, e^{\bar{q}\gamma}}{6(\bar{q}^2 - 3\bar{q} + 3)} \left(\frac{(2\bar{q} - 6)e^{(3-\bar{q})\gamma} - 2\bar{q}\, e^{-\bar{q}\gamma}}{\gamma} \right. \\ &\left. + \, 2\frac{e^{(3-\bar{q})\gamma} - e^{-\bar{q}\gamma}}{\gamma^2} + 9 - 6\bar{q} \right) + e^{\bar{q}\gamma}. \end{aligned}$$

In particular, for $\bar{q} = 0$ we get

$$A^{(3)} = A^{(5)}(0) = \frac{1}{18}\left(\frac{6e^{3\gamma}}{\gamma} - 2\frac{e^{3\gamma}-1}{\gamma^2} - 9\right),$$
$$B^{(3)} = B^{(5)}(0) = \frac{1}{18}\,e^{3\gamma}\left(\frac{6e^{-3\gamma}}{\gamma} + 2\frac{e^{-3\gamma}-1}{\gamma^2} + 9\right),$$

while for $\bar{q}$=3 we have

$$A^{(4)} = A^{(5)}(3) = \frac{1}{18}\,e^{3\gamma}\left(\frac{6e^{-3\gamma}}{\gamma} + 2\frac{e^{-3\gamma}-1}{\gamma^2} + 9\right),$$
$$B^{(4)} = B^{(5)}(3) = \frac{1}{6}\,e^{3\gamma}\left(\frac{6e^{-3\gamma}}{\gamma} + 2\frac{e^{-3\gamma}-1}{\gamma^2} + 9\right) + e^{3\gamma}.$$

From this it follows that two possible convex approximation of $\varphi_{i,j,w}(q)$ are

$$\varphi^{(\kappa)}_{i,j,w}(q) = \left(1 - \alpha\, A^{(\kappa)}\, q - \alpha\, B^{(\kappa)}\right)^2, \quad \kappa = 3, 4. \tag{11}$$

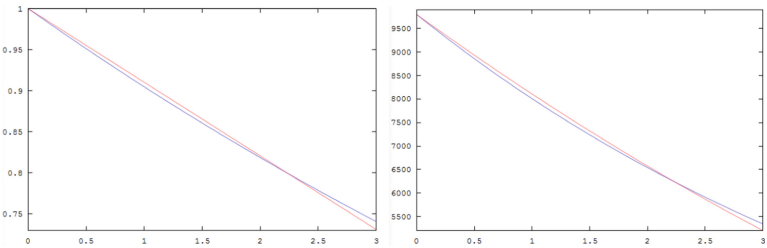

Fig. 3. On the left side: Graph of $g_{i,j,w}(q)$ in blue and $p^{(3)}(q)$ in red. On the right side: Graph of $\varphi_{i,j,w}(q)$ in blue and $\varphi^{(3)}(q)$ in red ($\alpha = 100$, $\gamma = 0.1$). (Color figure online)

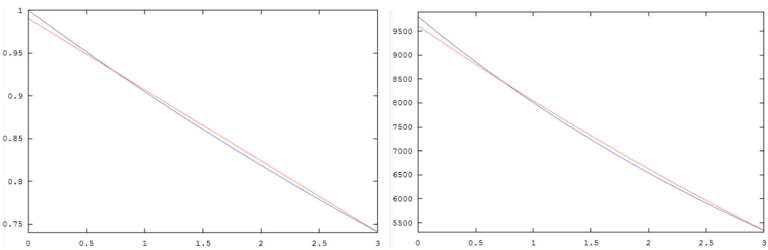

Fig. 4. On the left side: Graph of $g_{i,j,w}(q)$ in blue and $p^{(4)}(q)$ in red. On the right side: Graph of $\varphi_{i,j,w}(q)$ in blue and $\varphi^{(4)}(q)$ in red ($\alpha = 100$, $\gamma = 0.1$). (Color figure online)

6 The GNC Approximation Families

The first convex approximation of the consistency term of the energy function related to the interference level of the verso is expressed by

$$T^{(\kappa)}(s,q,A) = \sum_{i=1}^{n}\sum_{j=1}^{m}\sum_{w\in\{r,v\}} \psi(w)^d(i,j)\,\varphi^{(\kappa)}_{i,j,w}(q), \quad \kappa = 1,2,3,4. \tag{12}$$

We define the following families of functions of convex approximations. Let $T_p^{(\kappa)} = pT^{(\kappa)} + (1-p)T$. For $p = 1$, we get the first convex approximation associated with κ, while for $p = 0$ we have the original function T. Note that for $\kappa = 2$ we get the family of approximations used in the GNC-type algorithm proposed in [8] and [21].

7 Experimental Results

In this section we compare the experimental results, by using the four different GNC algorithms proposed in the previous sections. We have assumed two different pairs of original images, given in Figs. 5 and 6. We have used a uniform blur mask of dimension 5×5, and we have considered the interference levels to be estimated given in the Fig. 7. In this figure, if the interference value of a single pixel is 0, then that pixel is presented in black while, and if the interference value is 3 (that is very high), then that pixel is presented in white. The gray pixels represent interference values between 0 and 3. Observe that it is not possible to assume completely random interference levels, since they are supposed to be smooth. Thus, we tested our algorithms only by means of the proposed interference level in Fig. 7.

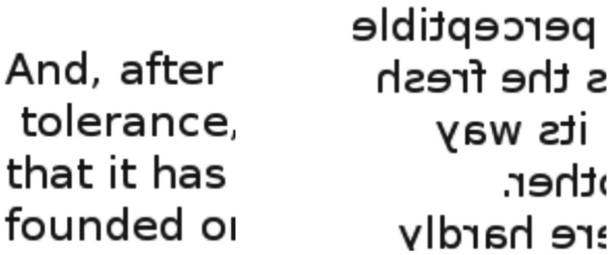

(a) (b)

Fig. 5. First pair of ideal sources

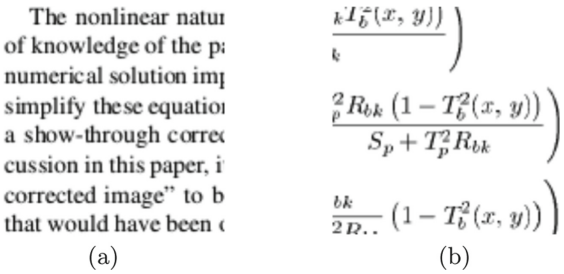

Fig. 6. Second pair of ideal sources

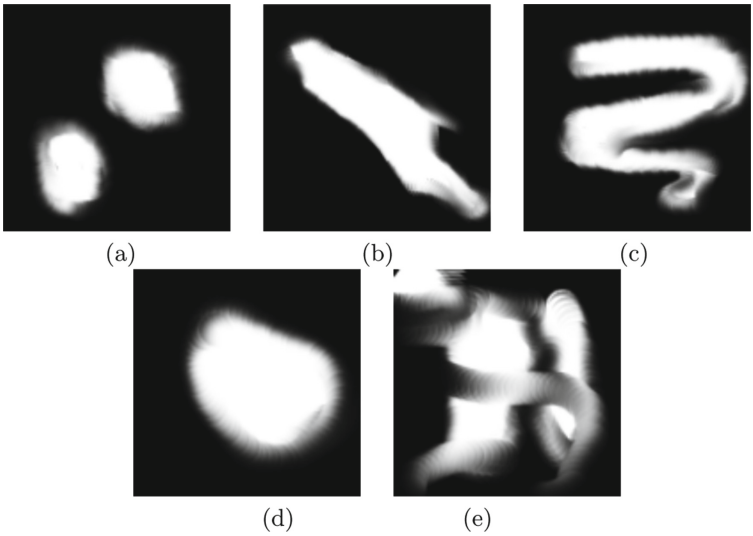

Fig. 7. Interference levels: (a) $q_f^{(1)} = q_r^{(1)}$; (b) $q_f^{(2)} = q_r^{(2)}$; (c) $q_f^{(3)} = q_r^{(3)}$; (d) $q_f^{(4)} = q_r^{(4)}$; (e) $q_f^{(5)} = q_r^{(5)}$.

Note that we have assumed that the ideal interference levels of the recto and of the verso coincide. Considering the first pair of original sources given in Fig. 5 and the interference levels given in Fig. 7, we obtain the data mixtures given in Fig. 8. We have tested the four GNC algorithms, assuming the following regularization parameters:

$$\lambda_f = \lambda_r = 50, \quad \lambda_c = 100.$$

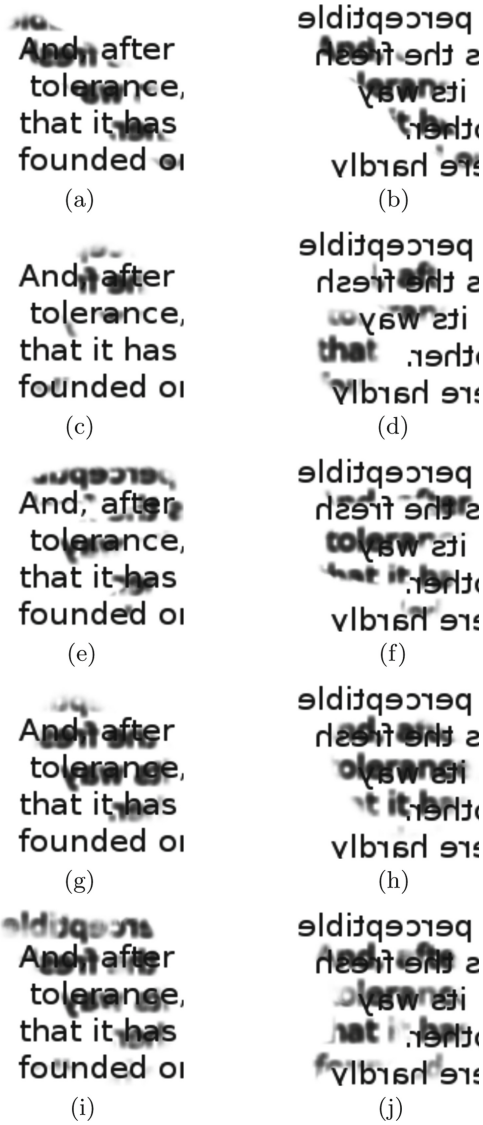

Fig. 8. (a–b) Document in Fig. 5 degraded by the interference level $q_r^{(1)} = q_v^{(1)}$; (c–d) document in Fig. 5 degraded by the interference level $q_r^{(2)} = q_v^{(2)}$; (e–f) document in Fig. 5 degraded by the interference level $q_r^{(3)} = q_v^{(3)}$; (g–h) document in Fig. 5 degraded by the interference level $q_r^{(4)} = q_v^{(4)}$; (i–j) document in Fig. 5 degraded by the interference level $q_r^{(5)} = q_v^{(5)}$.

We have compared the four proposed algorithms in terms of mean square error (MSE) between the estimate of the obtained interference level and the ideal interference level given in Fig. 7. In Table 1 there are the errors in terms of MSE obtained by the proposed algorithms, by considering the pair of original sources presented in Fig. 5 and the interference levels $q_f^{(i)} = q_r^{(i)}$, $i = 1, \ldots, 5$, given in Fig. 7. The effectiveness of the algorithm has been tested by using some images, created to highlight the capacity of the algorithm to eliminate the degradations due to the effect of show-through.

Table 1. MSE of the proposed algorithms, using the original sources in Fig. 5.

	$q_f^{(1)}$	$q_r^{(1)}$	$q_f^{(2)}$	$q_r^{(2)}$	$q_f^{(3)}$	$q_r^{(3)}$	$q_f^{(4)}$	$q_r^{(4)}$	$q_f^{(5)}$	$q_r^{(5)}$
$\kappa = 1$	0.0571	0.0533	0.0719	0.0831	0.0798	0.0784	0.0821	0.0792	0.1021	0.0987
$\kappa = 2$	0.0358	0.0374	0.0338	0.0412	0.0440	0.0398	0.0314	0.0267	0.0373	0.0417
$\kappa = 3$	0.0318	0.0400	0.0372	0.0394	0.04183	0.0427	0.0273	0.0264	0.0413	0.0398
$\kappa = 4$	**0.0214**	**0.0235**	**0.0232**	**0.0224**	**0.0314**	**0.0303**	**0.0098**	**0.0113**	**0.0352**	**0.0388**

The best results obtained in Table 1 are indicated in red. As it is possible to observe, the best algorithm for the first pair of images is associated to the family of approximations obtained with $\kappa = 4$. In Fig. 9 we present the interference levels estimated by the algorithm related to $\kappa = 4$.

Regarding the second pair of original sources in Fig. 6 and the interference levels in Fig. 7, and taking a uniform mask of type 5×5, we have the data mixtures in Fig. 10. We have tested the four GNC algorithms, using the previous regularization parameters. In Table 2 the errors in terms of MSE obtained by the proposed algorithms, by considering the pair of original sources presented in Fig. 6 and the interference levels $q_f^{(i)} = q_r^{(i)}$, $i = 1, \ldots, 5$, given in Fig. 7. In Table 2 the best results which we obtained are indicated in red. So it is possible to notice that in the 100% of the examined cases the algorithm which gives the best results is that corresponding with $\kappa = 4$.

As we see in Table 2, the best algorithm for the first pair of images is again that related to the family of approximations with $\kappa = 4$. In Fig. 11 there are the interference levels estimated by the algorithm corresponding with $\kappa = 4$.

Table 2. MSE of the proposed algorithms, using the original sources in Fig. 6.

	$q_f^{(1)}$	$q_r^{(1)}$	$q_f^{(2)}$	$q_r^{(2)}$	$q_f^{(3)}$	$q_r^{(3)}$	$q_f^{(4)}$	$q_r^{(4)}$	$q_f^{(5)}$	$q_r^{(5)}$
$\kappa = 1$	0.0523	0.0497	0.0613	0.0671	0.0942	0.0817	0.1218	0.1375	0.1129	0.1567
$\kappa = 2$	0.0337	0.0302	0.0363	0.0337	0.0479	0.0328	0.0371	0.0442	0.0385	0.0406
$\kappa = 3$	0.0315	0.0313	0.0332	0.0353	0.0318	0.0338	0.0418	0.0573	0.0397	0.0393
$\kappa = 4$	**0.0238**	**0.0252**	**0.0243**	**0.0254**	**0.0102**	**0.0175**	**0.0258**	**0.0323**	**0.0332**	**0.0358**

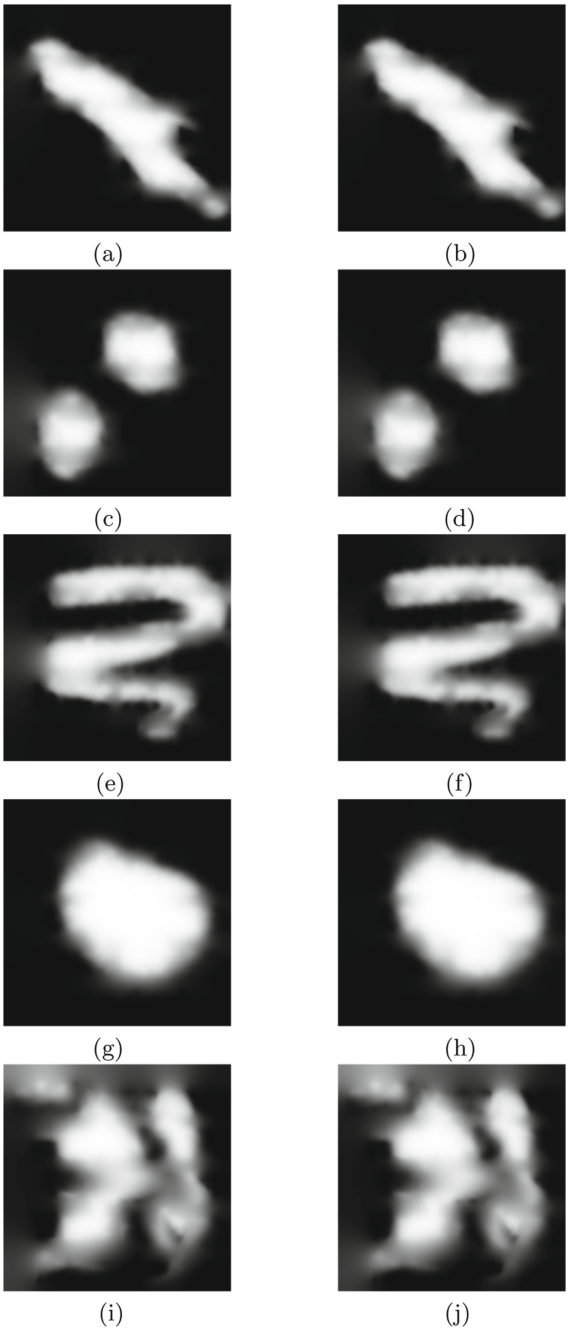

Fig. 9. (a) estimation of $q_f^{(1)}$; (b) estimation of $q_r^{(1)}$; (c) estimation of $q_f^{(2)}$; (d) estimation of $q_r^{(2)}$; (e) estimation of $q_f^{(3)}$; (f) estimation of $q_r^{(3)}$; (g) estimation of $q_f^{(4)}$; (h) estimation of $q_r^{(4)}$; (i) estimation of $q_f^{(5)}$; (j) estimation of $q_r^{(5)}$.

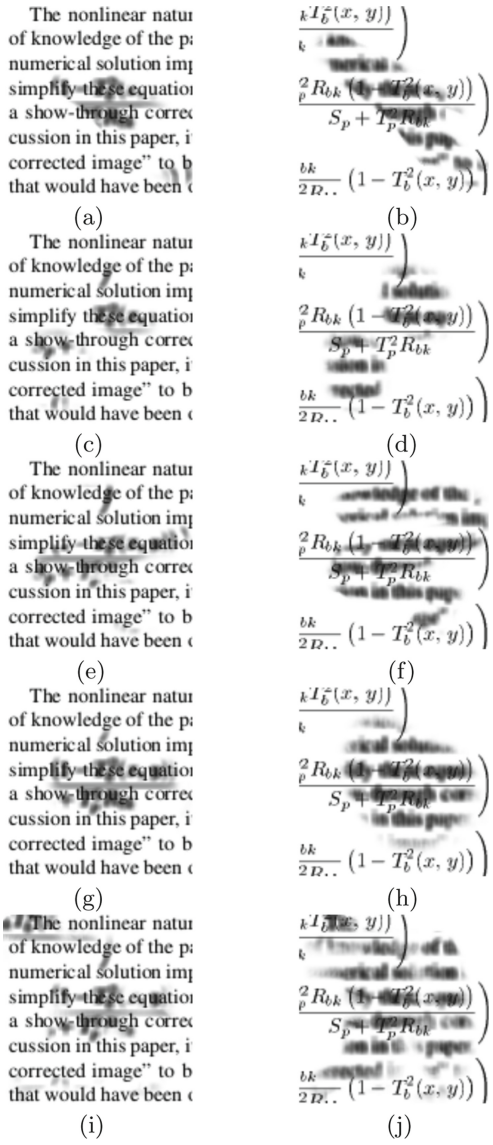

Fig. 10. (a–b) Document in Fig. 6 degraded by the interference level $q_r^{(1)} = q_v^{(1)}$; (c–d) document in Fig. 6 degraded by the interference level $q_r^{(2)} = q_v^{(2)}$; (e–f) document in Fig. 6 degraded by the interference level $q_r^{(3)} = q_v^{(3)}$; (g–h) document in Fig. 6 degraded by the interference level $q_r^{(4)} = q_v^{(4)}$; (i–j) document in Fig. 6 degraded by the interference level $q_r^{(5)} = q_v^{(5)}$.

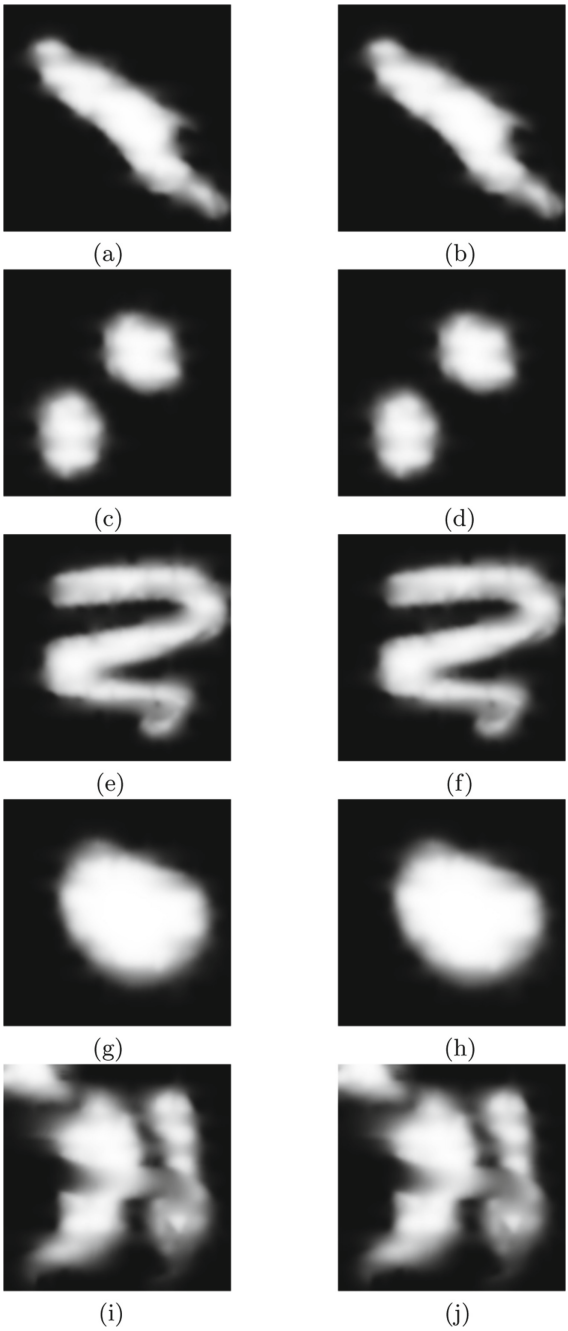

Fig. 11. (a) estimation of $q_f^{(1)}$; (b) estimation of $q_r^{(1)}$; (c) estimation of $q_f^{(2)}$; (d) estimation of $q_r^{(2)}$; (e) estimation of $q_f^{(3)}$; (f) estimation of $q_r^{(3)}$; (g) estimation of $q_f^{(4)}$; (h) estimation of $q_r^{(4)}$; (i) estimation of $q_f^{(5)}$; (j) estimation of $q_r^{(5)}$.

Thus, we propose to use the family of approximations given for $\kappa = 4$, improving the results obtained in [8] and [21], where the family of approximation with $\kappa = 2$ is used.

Conclusions

We studied the problem of blind separation of the components, in particular concerning ancient documents corrupted by bleed-through and show-through. We dealt with the problem of studying a regularization technique, which estimates the original sources, the interference levels and the blur operators. We investigated the estimate of the interference levels, given the original sources and the blur operators. In particular, we analyzed various GNC algorithms for minimizing the involved energy function. Such algorithms are different because of the choice of the first convex approximation. By means of the experimental results, we determined which algorithm gives more accurated estimates of the interference levels, improving the results given in [8] and [21]. In a forthcoming paper we will analyze the other steps of the technique here proposed, for the joint estimate of the original sources, the blur operator and the interference level.

Acknowledgment. This work was partially supported by University of Perugia, G.N.A.M.P.A. (Italian National Group of Mathematical Analysis, Probability and Applications) and I.N.d.A.M. (Italian National Institute of Higher Mathematics).

References

1. Bedini, L., Gerace, I., Tonazzini, A.: A deterministic algorithm for reconstruction images with interacting discontinuities. Comput. Vis. Graph. Image Process.: Graph. Models Images Process. **56**, 109–123 (1994)
2. Blake, A., Zisserman, A.: Visual Reconstruction. MIT Press, Cambridge, MA (1987)
3. Boccuto, A., Gerace, I.: Image reconstruction with a non-parallelism constraint. In: Proceedings of the International Workshop on Computational Intelligence for Multimedia Understanding, Reggio Calabria, Italy, 27–28 October 2016, IEEE Conference Publications, pp. 1–5 (2016)
4. Boccuto, A., Gerace, I., Giorgetti, V.: A blind source separation technique for document restoration. SIAM J. Imaging Sci. **12**(2), 1135–1162 (2019)
5. Boccuto, A., Gerace, I., Martinelli, F.: Half-quadratic image restoration with a non-parallelism constraint. J. Math. Imaging Vis. **59**(2), 270–295 (2017)
6. Boccuto, A., Gerace, I., Pucci, P.: Convex approximation technique for interacting line elements deblurring: a new approach. J. Math. Imaging Vis. **44**(2), 168–184 (2012)
7. Brewster, M.E., Kannan, R.: Nonlinear successive over-relaxation. Numerische Math. **44**(2), 309–315 (1984)
8. Gerace, I., Martinelli, F., Tonazzini, A.: Restoration of recto-verso archival documents through a regularized nonlinear model. In: Proceedings of 20th European Signal Processing Conference EUSIPCO, pp. 1588–1592 (2012)

9. Gerace, I., Palomba, C., Tonazzini, A.: An inpainting technique based on regularization to remove bleed-through from ancient documents. In: 2016 International Workshop on Computational Intelligence for Multimedia Understanding (IWCIM), pp. 1–5 (2016)
10. Hazan, E., Levy, K.Y., Shalev-Shwartz, S.: On graduated optimization for stochastic non-convex problems. In: Proceedings of the 33rd International Conference on Machine Learning, New York, NY, USA, 2016. JMLR: W& CP 48, pp. 1–9 (2016)
11. Khan, M.R., Imtiaz, H., Hasan, M.K.: Show-through correction in scanned images using joint histogram. SIViP **4**(3), 337–351 (2010)
12. Martinelli, F., Salerno, E., Gerace, I., Tonazzini, A.: Nonlinear model and constrained ML for removing back-to-front interferences from recto-verso documents. Patt. Recogn. **45**, 596–605 (2012)
13. Mobahi, H., Fisher, J.W.: A theoretical analysis of optimization by Gaussian continuation. In: Wong, W.-K., Lowd, D. (eds.) Proceedings of the Twenty-Ninth Conference on Artificial Intelligence of the Association for the Advancement of Artificial Intelligence (AAAI), Austin, Texas, USA, 25–30 January 2015, pp. 1205–1211 (2015)
14. Nikolova, M.: Markovian reconstruction using a GNC approach. IEEE Trans. Image Process. **8**(9), 1204–1220 (1999)
15. Nikolova, M., Ng, M.K., Tam, C.-P.: On ℓ_1 data fitting and concave regularization for image recovery. SIAM J. Sci. Comput. **35**(1), A397–A430 (2013)
16. Nikolova, M., Ng, M.K., Zhang, S., Ching, W.-K.: Efficient reconstruction of piecewise constant images using nonsmooth nonconvex minimization. SIAM J. Imaging Sci. **1**(1), 2–25 (2008)
17. Ophir, B., Malah, D.: Show-through cancellation in scanned images using blind source separation techniques. In: Proceedings of IEEE International Conference on Image Processing (3), pp. 233–236 (2007)
18. Robini, M.C., Magnin, I.E.: Optimization by stochastic continuation. SIAM J. Imaging Sci. **3**(4), 1096–1121 (2010)
19. Salerno, E., Martinelli, F., Tonazzini, A.: Nonlinear model identification and see-through cancelation from Recto/Verso data. Int. J. Document Anal. Recogn. (IJDAR) **16**(2), 177–187 (2013)
20. Sharma, G.: Show-through cancellation in scans of duplex printed documents. IEEE Trans. Image Process. **10**, 736–754 (2001)
21. Tonazzini, A., Gerace, I., Martinelli, F.: Document image restoration and analysis as separation of mixtures of patterns: from linear to nonlinear models. In: Gunturk, B.K., Li, X. (eds.) Image Restoration - Fundamentals and Advances, pp. 285–310. CRC Press, Taylor & Francis, Boca Raton (2013)
22. Tonazzini, A., Savino, P., Salerno, E.: A non-stationary density model to separate overlapped texts in degraded documents. SIViP **9**(1), S155–S164 (2014). https://doi.org/10.1007/s11760-014-0735-3